Потреба в гартованій та відпущеній сталі, особливо для виготовлення компонентів бойових машин, зросла. Ця сталь класифікується як високоміцна, тверда і кулененепробивна (броньова сталь). Підтримання стабільності твердості сталі дуже важливе, адже твердість є стандартом якості для броньової сталі. Висока твердість призводить до зростання крихкості, тому для її зменшення необхідний відпуск (залишкова напруга знімається відпуском). Температура аустеніту і відпуску впливають на твердість і зносостійкість гартованої та відпущеної сталі. Твердість і зносостійкість можливо отримати завдяки впливу гартування і відпуску на гарячекатану листову сталь в якості броньової сталі. Матеріалом, використаним в даному дослідженні, є гарячекатана листова сталь, виготовлена в Індонезії з вмістом вуглецю 0,29 %. Використовуваний метод полягає в нагріванні матеріалу до 900, 885 і 870 °C (витримка протягом 45, 30 і 15 хвилин) та охолодженні у воді. Гартовану сталь нагрівають до 150 °C (витримують протягом 45, 30 і 15 хвилин) і охолоджують на атмосферному повітрі. Були використані оптимальні параметри термообробки, методи Тагуті і дисперсійний аналіз. За обраними параметрами і рівнем термообробки можна дізнатися кількість необхідних зразків. Параметр термообробки впливає на твердість, а дисперсійний аналіз – на зносостійкість. Оптимальна твердість і зносостійкість становлять 566,48 HVN (±532 BHN) і 2,01×10^{-9} мм^2/кг відповідно. На обидва впливає температура аустеніту і відпуску

Ключові слова: тріщина, пластичність, твердість, витримка, мартенсит, гартування, міцність, відпуск, в'язкість, зносостійкість

UDC 669.13.018
DOI: 10.15587/1729-4061.2019.156799

EFFECT OF QUENCH AND TEMPER ON HARDNESS AND WEAR OF HRP STEEL (ARMOR STEEL CANDIDATE)

Yurianto
Master of Technical Sciences, Associate Professor*
E-mail: yurianto@undip.ac.id
Pratikto
Doctor of Technical Sciences, Professor*
E-mail: prayone_adi@ub.ac.id
Rudy Soenoko
Doctor of Technical Sciences, Professor*
E-mail: rudysoen@ub.ac.id
Wahyono Suprapto
Doctor of Technical Sciences, Professor*
E-mail: wahyos@ub.ac.id
*Department of Mechanical Engineering
Brawijaya University
Jl. Mayjen Haryono, 167, Malang, Indonesia, 65145

1. Introduction

High-strength and hardness steel is often used to make bullet-resistant components of military need. The limits for bullet-resistant steel (armor steel) are unclear, and hardness is important [1, 2]. Quenched and tempered (Q&T) steels are used in military applications due to high hardness, high strength to weight ratio, and excellent toughness [3]. Armor steel that has the highest ballistic resistance is AISI 4340 with a hardness of 50 HRC=485 BHN [4]. Keeping hardness stability is essential because this is a quality standard for armor steels. High hardness causes brittleness increase, and tempers are needed to increase ductility (residual stress is relieved by temper). The austenite and temper temperature will affect the Q&T Steel hardness and wear resistance. Then the use of the optimum austenite and temper temperature is very important to obtain the hardness and wear of quenched and tempered steel.

So far, no researcher has examined the optimization of quench and tempering heat treatment parameters against hardness and wear. This research is an attempt to obtain hardness and wear that are influenced by austenite temperature, austenite holding time, and temper holding time. So this is the novelty of this research.

2. Literature review and problem statement

Coarse austenites are obtained at the higher austenite temperature because of grain growth, and quenching produces coarse martensite. The austenite temperature is closest to Ar_3, the fine martensite is produced and expressed by [5],

$$\mathrm{Ar_3} = (\mathrm{C}) \approx 910-(310\mathrm{C})-(80\mathrm{Mn})- \\ -(80\mathrm{Mo})-(55\mathrm{Ni})-(20\mathrm{Cu})-(15\mathrm{Cr}). \quad (1)$$

Austenite transforms to martensite at the end of the quench. Martensite starts to form at temperature M_s and finishes at temperature M_F, and both temperatures are expressed by [6],

$$M_s(\mathrm{C}) \approx 561-(474\mathrm{C})-(33\mathrm{Mn})- \\ -(17\mathrm{Ni})-(17\mathrm{Cr})-(21\mathrm{Mo}). \quad (2)$$

$$M_F(\mathrm{C}) = 175\ ^\circ\mathrm{C} - 165\ ^\circ\mathrm{C}\ \text{below}\ \mathrm{M_s}. \quad (3)$$

Ductility of quenched steel can be increased using temper, and quenched and tempered steels are produced. Tempering temperature, which reduces the residual stress due to previous quenching, is 150 °C [7]. Wear is related to hardness, fracture resistance, and thermal stability for

Received date: 19.02.2019 Accepted date: 23.05.2019 Published date: 30.06.2019

high-temperature wear [8]. Increased carbon concentration systematically lowers M_s temperature and increases alloy hardness [9]. By transforming lath sub-structure bainite into cells at high tempering temperature, the fine grains are produced [10]. The hardness decreases with increasing temper temperature, which produces a corresponding increase in penetration depth [11]. With the addition of carbon elements, the tensile strength increases with a slight increase in martensite transformation temperature. Broader distribution of martensite in good auto-tempered steel can help ductility increase by increasing work-hardenability during tension [12]. While at higher austenitization temperatures and longer austenitization times, the larger grains are produced [13]. Martensite abrasion is not guaranteed compared to lower hardness, which has better ductility. The brittle martensite properties have lower wear resistance [14]. Heat treated steel improves its service conditions, especially in creep resistance [15] and is suiTable for continuous heat exposure. The contribution of strength is because the dislocation density is higher than the strengthening precipitation of tempered martensite. Samples that were rapidly tempered contributed to higher precipitation strength than tampered slowly [16].

The martensite carbon content depends on the volume of ferrite and martensite fractions developed as a transformation result of the ferrite and martensite phases after successful immersion and quenching [17]. Because the dislocation density and martensite carbon content decrease due to temper, the martensite strength decreases. The remaining residual strain is indicated by mean kernel misorientation, which is allowed by reorganization or destruction of dislocation geometrically [18].

The micro-spherical structure shows resistance to wear. Therefore, spheroidized heat treatment processes can be used to reduce wear in ultra-high carbon steel [19]. High-carbon martensite steel has poor ductility [20]. Smoother surfaces produce a lower coefficient of friction [21]. The fine grain structure produces a smooth surface and ductility increases, and wear resistance increases. The specific wear is calculated by the following for formula [22],

$$SW = \frac{B \times B_o^2}{8r \times P_o \times L_o}, \tag{4}$$

where B – width of the rotating disk; B_o – length of wear; r – radius of the disk; P_o – load given; L_o – abrasion distance.

The resistance of materials to indentation is hardness, and Vickers and Brinell hardness number – *BHN* is used in this research.

The Taguchi methods are used to improve product quality and processes. At the same time, this method can reduce the costs and the resources as low as possible, and they are strong to the disturbance factor. Processing of data is made using equations (5) to (20) [23, 24]. The first step is to create a design that includes a combination of parameters and levels and the determination of orthogonal matrices. For more accurate data of each parameter, two replications are made. The orthogonal matrix (OM) is determined by the following formula,

$$OM = L_a b^c, \tag{5}$$

where L – symbol of the orthogonal matrix; a – number of experiments; b and c – level and control factor, respectively.

The second step is to interpret the tested data by calculating the response ratio with the following equation.

For hardness, Larger the better (LTB),

$$\frac{S}{n} ratio = -10\log_{10}\left[\frac{1}{n}\sum_{i=1}^{n}\frac{1}{y_i^2}\right]. \tag{6}$$

For specific resistance, Smaller the better (STB) is expressed,

$$\frac{S}{n} ratio = -10\log_{10}\left[\frac{1}{n}\sum_{i=1}^{n} y^2\right], \tag{7}$$

where $\frac{S}{n}$ ratio – signal to noise ratio; y – response value.

The $\frac{S}{n}$ ratio shows how strong the test parameters are in interference. The higher the $\frac{S}{n}$ ratio the strongest their parameters and the results can be used to strengthen for average response data.

ANOVA calculations include calculation of the sum of the total error and parameters level n and use the following equations (8) to (11) [23, 24],

$$S_t = \sum R^2; \tag{8}$$

$$S_m = n \times \overline{R}^2; \tag{9}$$

$$S_p = \frac{[L_1]^2}{n_{A_1}} + \frac{[L_2]^2}{n_{A_2}} + \frac{[L_3]^2}{n_{A_3}} - \frac{[T]}{N}; \tag{10}$$

$$S_e = S_t - S_m - S_p, \tag{11}$$

where S_t – sum of the total square; S_m – sum of the square mean; S_p – sum of the square parameter; L – level, T – sum of average data; S_e – sum of the total error.

Contribution values (pA %) for each parameter to response are calculated using equations (12) to (15) [23, 24],

$$MS = \frac{SA}{S_e}; \tag{12}$$

$$F_{ratio} = \frac{MS}{S_e}; \tag{13}$$

$$SA' = S_A - vA \times Ve; \tag{14}$$

$$pA(\%) = \frac{SA'}{S_t} \times 100\,\%, \tag{15}$$

where MS – average square response; vA – degree of freedom; Ve – varian (σ^2); SA' – actual number of the squares of the factor.

To conclude the parameter effect on the response and essential parameters in calculating the optimal response predictive, ANOVAs are used. If $F_{ratio} > F_{total}$, the parameter does not have a significant effect on the response and vice versa.

The optimal predictive value and confidence interval (CI) of the research are calculated by equations,

$$n_{eff} = \frac{\text{sum of total experiment}}{1 + \text{sum of prediction degree of freedom}};$$

$$CI = \sqrt{\frac{F_{\alpha,v_1,v_2} \times Ve}{n_{eff}}}, \quad (16)$$

where α – level of confidence; v_1 – quantifier of trust for the degree of freedom. v_2 – denominator of pool error for the degree of freedom.

3. The aim and objectives of the study

The study aims to obtain hardness and wear due to the influence of quench and temper on hot rolled plate steel as the armor steel candidate.

The following objectives achieve the aim accomplished:

– select heat treatment parameters and level, hardness and wear, and arranged in an orthogonal matrix and its levels;

– determine hardness and wear based on heat treatment parameter optimization;

– interpretation of austenite, holding time, and temper has an influence on hardness and wear.

4. Material and method of the research

4. 1. Material

The material used during the research was hot rolled steel (raw material of quenched and tempered steels.) made by PT. Krakatau Steel (Persero), Cilegon, Banten Province, Indonesia. This material was produced in 2008. Generally, this steel is used to make components that need high hardness and strength.

4. 2. Method of the research

The heat treatment parameters used are the austenite temperature (A), austenite holding time (B), and tempering temperature (C). While the response used are hardness and wear (both hardness and wear were carried out in two replications) before and after heat treatment condition. All of them are arranged in an orthogonal matrix.

Equations (4)–(16) were used to determine the hardness, wear, and heat treatment parameters (including levels), then processed using Minitab 18 software.

The cooling media used in quenching heat treatment is water because easily controlled, comforTable to obtain and the cheapest than the other, and influence on wear and impact.

The nine specimens each were heated as follows: 870 °C (holding time 15 minutes); 870 °C (holding time 30 minutes); 870 °C (holding time 45 minutes); 885 °C (holding time 15 minutes); 885 °C (holding time 30 minutes); 885 °C (holding time 45 minutes); 900 °C (holding time 15 minutes); 900 °C (holding time 30 minutes); 900 °C (holding time 45 minutes). Then each specimen was quenched in a water medium. After quenching, heating was carried out at 150 °C and held for 30 minutes for each specimen. Heating was carried out using a NABERTHERM heating furnace with a maximum temperature of 1100 °C.

Each specimen was tested using microhardness Vickers ZWICK Type Zhu and Ogoshi wear testing machines made by Tokyo Testing machines.

5. Results of the research

Observation of the chemical elements contained in HRP Steel is shown in Table 1. Temperatures Ar_3, M_s and M_F are determined by the formula (1) to (3) and shown in Table 2.

Table 1

Chemical elements of HRP Steel

Element	C	Cr	Cu	Mn	Mo	Ni	Fe
% weight	0.29342	0.55029	0.08337	1.41218	0.19303	0.27877	97.18894

Table 2

Temperature, hardness and wear of HRP Steels

Ar_3	M_s	M_F	Hardness	SW
765 °C	357 °C	182 °C to 192 °C	288 HVN (273 BHN)	$7.34\times10^{-9}\ \frac{mm^2}{kg}$

Based on equation (5), heat treatment parameters and responses in the orthogonal matrix L_9 (3^4) for hardness, average hardness, and hardness to levels are shown in Tables 3, 4, respectively. Minitab processes Tables 3, 4 and Fig. 1 was obtained. $\frac{S}{n}$ of hardness ratio and $\frac{S}{n}$ of average hardness and $\frac{S}{n}$ ratio of hardness to level parameters are shown in Tables 5, 6, respectively, and using Minitab Fig. 2 was obtained.

The results of ANOVA calculation for hardness are shown in Tables 7, 8.

Wear, average wear and wear to levels are shown in Tables 9, 10 respectively. Average specific wear to level parameters are shown in Fig. 3. The results of $\frac{S}{n}$ for specific wear and average $\frac{S}{n}$ ratio for specific wear are shown in Table 11 and Table 12, respectively. Average $\frac{S}{n}$ ratio of specific wear to level parameters is shown in Fig. 4. The results of the calculation by ANOVA for specific wear are shown in Tables 13, 14.

Table 3

Hardness

Specimen	A	B	C	H_A	H_B	H_C
1	870	15	125	571	552	561
2	870	30	150	533	533	542
3	870	45	175	551	533	524
4	885	15	150	524	533	533
5	885	30	175	515	505	490
6	885	45	125	542	542	551
7	900	15	175	515	515	515
8	900	30	125	571	581	571
9	900	45	150	542	551	542

Table 4

Average hardness

Level	A	B	C
1	544.44	535.44	560.11
2	526.00	537.89	537.00
3	544.78	541.89	518.11
Difference	18.78	6.44	42.00
Rank	2	3	1

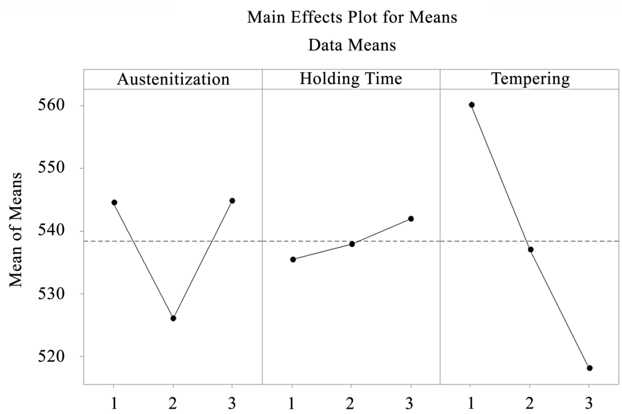

Fig. 1. Graph of average hardness to level parameters

Table 5

$\frac{S}{n}$ hardness ratio

Specimen	A	B	C	$ratio\frac{S}{n}$
1	870	15	125	54.9819
2	870	30	150	54.5825
3	870	45	175	54.5776
4	885	15	150	54.4847
5	885	30	175	54.0316
6	885	45	125	54.7217
7	900	15	175	54.2361
8	900	30	125	55.1824
9	900	45	150	54.7271

Table 6

Average $\frac{S}{n}$ ratio of hardness

Level	A	B	B
1	54.7140	54.56758	54.96202
2	54.4127	54.59885	54.5981
3	54.7152	54.67551	54.28181
Difference	0.3025	0.1079	0.6802
Rank	2	3	1

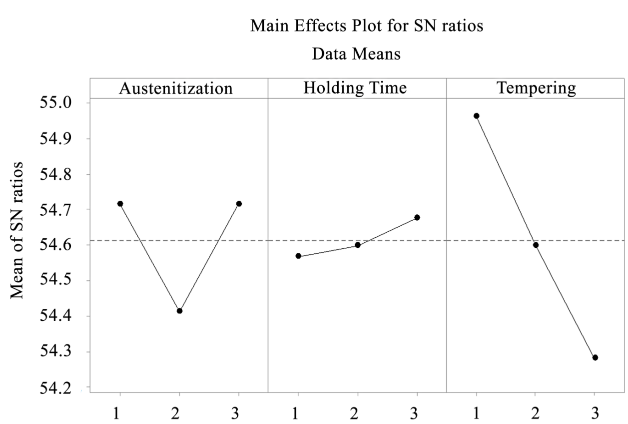

Fig. 2. Graph of average $\frac{S}{n}$ ratio of hardness to level parameters

Table 7

ANOVA of Hardness

Source	S_{source}	vA	M_{source}	F_{ratio}	F_{total}	$pA\%$
Austenitize (A)	2078.74	2.00	1039.37	9.41	3.49	16.71
Holding (B)	190.52	2.00	95.26	0.86	3.9	1.53
Tempering (C)	7964.74	2.00	3982.37	36.06	3.49	64.01
Pool Error	2208.52	20.00	110.43	–	–	17.75
Total-1	12442.52	–	–	–	–	100.00

Table 8

Updated ANOVA of Hardness

Source	S_{source}	vA	M_{source}	F_{ratio}	F_{total}	$pA\%$
Austenitize (A)	2078.74	2.00	1039.37	9.41	3.49	16.71
Tempering (C)	7964.74	2.00	3982.37	36.06	3.49	64.01
Pool. Error	2399.04	22.00	205.69	–	–	19.28
Total-1						100

Table 9

Specific wear Test Results

Specimen	Replication		Average Specific Wear $\frac{mm^2}{kg}$
	SW_1	SW_2	
1	2.11×10^{-9}	2.46×10^{-9}	2.28×10^{-9}
2	1.95×10^{-9}	2.11×10^{-9}	2.03×10^{-9}
3	2.28×10^{-9}	1.95×10^{-9}	2.11×10^{-9}
4	2.85×10^{-9}	2.85×10^{-9}	2.85×10^{-9}
5	2.46×10^{-9}	2.65×10^{-9}	2.55×10^{-9}
6	1.95×10^{-9}	2.46×10^{-9}	2.20×10^{-9}
7	2.65×10^{-9}	3.05×10^{-9}	3.85×10^{-9}
8	3.05×10^{-9}	2.65×10^{-9}	2.85×10^{-9}
9	4.80×10^{-9}	2.38×10^{-9}	3.54×10^{-9}

Table 10

Average Specific Wear to Level Parameters

Level	Austenitiza-tion (A)	Holding time	Tempering
1	2.14×10^{-9}	2.66×10^{-9}	2.45×10^{-9}
2	2.53×10^{-9}	2.48×10^{-9}	2.80×10^{-9}
3	3.08×10^{-9}	2.62×10^{-9}	2.51×10^{-9}
Difference	0.94×10^{-9}	0.18×10^{-9}	0.35×10^{-9}
Rank	1	3	2

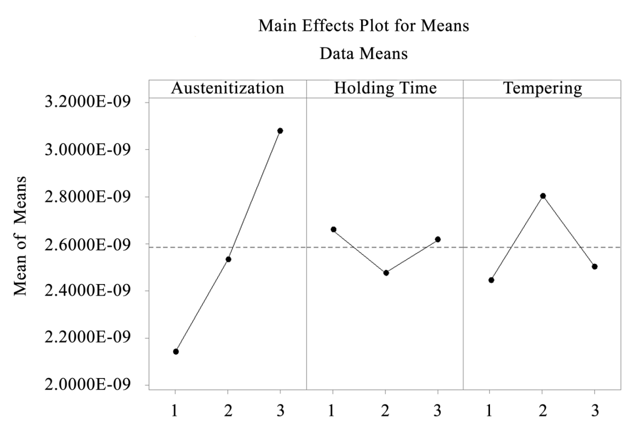

Fig. 3. Graph of average Specific Wear to Level Parameters

Table 11

Results of calculation of $\frac{S}{n}$ specific wear

Specimen	Replication		$\frac{S}{n}$ ratio
	SW_1	SW_2	
1	2.11×10^{-9}	2.46×10^{-9}	172.80
2	1.95×10^{-9}	2.11×10^{-9}	173.86
3	2.28×10^{-9}	1.95×10^{-9}	173.48
4	2.85×10^{-9}	2.85×10^{-9}	170.92
5	2.46×10^{-9}	2.65×10^{-9}	171.85
6	1.95×10^{-9}	2.46×10^{-9}	173.08
7	2.65×10^{-9}	3.05×10^{-9}	170.88
8	3.05×10^{-9}	2.65×10^{-9}	170.88
9	4.80×10^{-9}	2.38×10^{-9}	168.50

Table 12

Average $\frac{S}{n}$ ratio for specific wear

Level	*A*	*B*	*C*
1	173.4	171.5	172.3
2	172.0	172.2	171.1
3	170.1	171.7	172.1
Difference	3.3	0.7	1.2
Rank	1	3	2

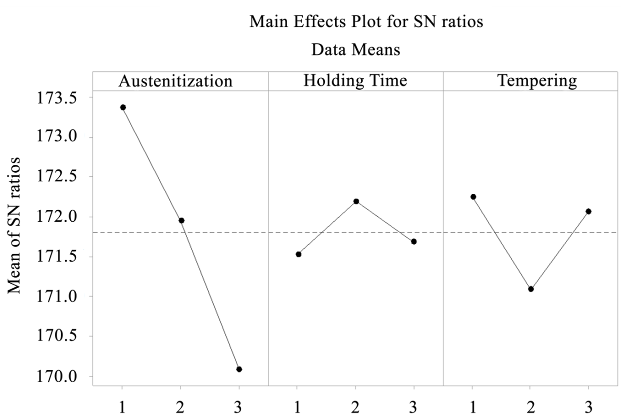

Fig. 4. Graph of the average ratio $\frac{S}{n}$ of specific wear to Level Parameters

Table 13

ANOVA of specific wear

Source	S_{source}	vA	M_{source}	F_{ratio}	F_{total}	$pA\%$
Austenitization (A)	1.33×10^{-18}	2.00	6.68×10^{-19}	26.09	3.98	70.37
Holding (B)	5.52×10^{-20}	2.00	2.76×10^{-20}	1.08	3.98	2.92
Tempering (C)	2.22×10^{-19}	2.00	1.11×10^{-19}	4.33	3.98	11.75
Error	2.82×10^{-19}	11.00	2.56×10^{-20}	–	–	14.96
Total-1	18.89×10^{-19}	17.00	–	–	–	100.00

Table 14

Updated ANOVA of specific wear

Source	S_{source}	νA	M_{sorce}	F_{ratio}	F_{total}	$pA\%$
Austenitization (A)	1.33×10^{-18}	2.00	6.68×10^{-19}	26.09	3.98	70.37
Tempering (C)	2.22×10^{-19}	2.00	1.11×10^{-19}	4.33	3.98	11.75
Pooled Error	3.37×10^{-19}	13.00	5.32×10^{-20}	–	–	17.88
Total-1	12.00×10^{-9}	17.00	–	–	–	100.00

6. Discussion of experimental results

6. 1. Hardness

Based on ranking, the effect of heat treatment parameters on hardness is temper temperature, austenitization and holding time (Tables 4, 6 and Fig. 1).

Martensite and residual stresses are produced together by previous quenching. Martensite hardness is increased metallurgically. Residual stress increasing the hardness mechanically due to the dense microstructure but increases crack susceptibility and needs to be reduced. The residual stress can be released by a tempering temperature of 150 °C because there is no martensite diffusion by temper heat (because it is still below M_F=182 °C to 192 °C). If the tempering temperature is above the martensite finish temperature, the hardness will be reduced by temper heat activation.

The second rank is austenite temperature. The hardness of 544.44 HVN=512 BHN and decreased at level 2 (526 VHN=495 BHN) and highest hardness (544.78 VHN= =512 BHN). Level 1, 2 and 3 have a slightly increased hardness (and ununiform hardness is produced). Nonuniform hardness due to unsTable austenite temperature consequently is the ununiform austenite structures, and ununiform martensite is produced.

The third rank is holding time. Level 1 producing 535.44 VHN and increase to 537.89 VHN=506 BHN (at level 2). At level 3 producing 541.89 VHN=510 BHN (highest hardness). Holding for a longer time will decrease the hardness because of martensite diffusion. The pattern of hardness influenced by austenite temperature, the higher the temperature will produce coarse austenite. Austenite holding time and tempering temperature have the same trend.

Temper temperature is the heat treatment parameter most influencing hardness. Hardness slightly decreases by the release of residual stress and ductility increases.

From the ANOVA of hardness, the contribution of heat treatment parameters (austenitization, holding, and tempering) is shown in Table 6 and Table 7. Austenite temperature, holding time and temper temperature have contributed to the hardness of steels, namely:

1) A factor of austenite temperature. $F_{calculate}$ (9.41)> >F_{total} (3.49). Then H_1 is accepted, meaning there is an effect of austenite temperature on steel hardness.

2) Factor of holding time. $F_{calculate}$ (0.86)<F_{total} (3.49). Then H_1 is rejected, meaning there is no effect of holding time on steel hardness.

3) Factor of t*empering temperature*. F_{hitung} (27.88)>F_{total} (3.49). Then H_1 is accepted, meaning there is an influence of *tempering temperature* on steel hardness.

From the data above, the predictive value of hardness and the confidence interval for measuring the deviation of the predicted value can be calculated. Hardness predictions are calculated using equations (14)–(16) as follows.

Hardness prediction

$$H_p = 538.41 + (A_3 - 538.41) + (C_1 - 538.41);$$

$$H_p = 538.41 + (544.78 - 538.41) + (560.11 - 538.41);$$

$$H_p = 566.48\ \text{VHN} \approx 532\ \text{BHN}.$$

Efficiency for hardness

$$n_{eff}=\frac{27}{2+2+2}=4.5.$$

Confidence interval for hardness

$$CI=\sqrt{\frac{3.49\times 205.69}{4.5}}=12.63\ \text{VHN}=13\ \text{BHN}.$$

Hardness

$$H=H_p\pm CI;$$

$$H_p=566.48\ \text{VHN}\approx 532\ \text{BHN};$$

$$H=(566.48\pm 12.63)\,\text{VHN}\approx(532\pm 13)\ \text{BHN}.$$

In data processing, take level three because the minimum level is permitted. Another consideration is seeing the trend of hardness after the heat treatment process. For industry is done by scaling because of the significant specimen need for concern. The response value for hardness changes due to the heat treatment parameters and level are used.

6. 2. Specific wears

Based on ranking, the effect of heat treatment parameters on wear is austenitization, tempering temperature and holding time (Tables 10, 12 and Fig. 3).

The higher the austenite temperature, the coarser austenite grain size will be produced (the coarser the austenite the harder and more brittle martensite will be produced when quenching is finished). If the quench is held as close as possible to Ar_3 (still above Ar_3), the fine martensite grain structure will be obtained. High hardness causes brittle material and decrease in specific wear. So, specific wear needs hardness and ductility.

The second rank is temper temperature. Specific wear fluctuating $2.45\times10^{-9}\ \frac{\text{mm}^2}{\text{kg}}$ goes up to level two $2.80\times10^{-9}\ \frac{\text{mm}^2}{\text{kg}}$ and goes down to level three $2.51\times10^{-9}\ \frac{\text{mm}^2}{\text{kg}}$. Specific wear fluctuations are caused by changes in time for tempering. Tempering temperature increases the decrease in specific wear.

The third rank is holding time, and the specific wear decreases slightly. Possible decrease in hardness causes the fact that the structure is not sTable yet during the holding, and these structures need enough time to reach a sTable condition. STable conditions will improve steel ductility (in this case, in quenched and tempered steel). STable condition is the structures that do not move when heating during the holding time.

The ANOVA for specific wear, austenitization, holding and tempering are shown in Tables 13, 14. Heat treatment parameter has contributed to the specific wear of steel, namely:

1. Factor of austenite temperature. $F_{ratio}(26.09)>F_{total}(3.98)$. Then H_1 is accepted, meaning there is a significant effect of austenite temperature on specific wear of hot rolled plate steel.

2. Factor of holding time. $F_{ratio}(1.08)<F_{total}(3.98)$. Then H_1 is rejected, meaning there is no sign of holding time effect on specific wear of hot rolled plate steel.

3. Factor of tempering temperature. $F_{ratio}(4.33)<F_{total}(3.98)$. The H_1 is accepted, meaning there is a significant influence on specific wear of hot rolled plate steels.

From the data above, the predictive value of specific wear and the confidence interval for measuring the deviation of the predicted value were determined. Specific wear predictions were determined using equations (14)–(16) as follows.

Specific wear prediction

$$SW_p=2.58\times10^{-9}+\left(2.14\times10^{-9}-258\times10^{-9}\right)+$$
$$+\left(2.45\times10^{-9}-2.58\times10^{-9}\right);$$

$$SW_p=2.01\times10^{-9}\ \frac{\text{mm}^2}{\text{kg}}.$$

Efficiency for specific wear

$$n_{eff}=\frac{18}{2+2+2}=3.6.$$

Confidence interval for specific wear

$$CI=\sqrt{\frac{3.98\times5.32\times10^{-20}}{36}}=2.42\times10^{-10}.$$

Specific wear

$$SW_p=(2.01\pm0.242)\times10^{-9}\ \frac{\text{mm}^2}{\text{kg}}.$$

Specific wear response values change because of the heat treatment parameters and levels used.

7. Conclusions

The research activities have completed and can be summarized as follows.

1. The orthogonal matrix with three levels to optimize the heat treatment parameters for wear and tear is L_9 (3^4). This matrix is sufficient to determine the contribution of heat treatment parameters to hardness and wear. The heat treatment parameters most influencing hardness and wear are the austenite temperature at level 3 (at 900 °C) and tempering temperature at level 1 (150 °C).

2. Optimization for hardness and wear is predicted to be around 566.48±12.63 HVN=(532±13) BHN and $(2.01\pm0.242)\times10^{-9}\ \frac{\text{mm}^2}{\text{kg}}$, respectively.

3. The closest the austenite temperature to the Ar_3 line, the most refined austenite structure is, and fine martensite is produced when the quenching is finished. The fine grain structure will increase ductility. Ductility is increased by tempering at 150 °C, this temperature releases residual stress only, and there is no martensite diffusion. The holding time to obtain structural stability during austenite heating and tempering and a Table structure on warming will produce a homogenous microstructure.

Acknowledgments

The author would like to thank Pradika Andarisa (Mechanical Engineer) for his technical assistance. This assistance in the preparation of the optimal calculation using Minitab 18 in this article is gratefully acknowledged.

Reference

1. Madhusudhan Reddy G., Mohandas T., Papukutty K. Enhancement of ballistic capabilities of soft welds through hardfacing // International Journal of Impact Engineering. 1999. Vol. 22, Issue 8. P. 775–791. doi: https://doi.org/10.1016/s0734-743x(99)00020-2
2. Dynamic fracture toughness of armour grade quenched and tempered steel joints fabricated using low hydrogen ferritic fillers / Magudeeswaran G., Balasubramanian V., Sathyanarayanan S., Reddy G. M., Moitra A., Venugopal S., Sasikala G. // Journal of Iron and Steel Research International. 2010. Vol. 17, Issue 5. P. 51–56. doi: https://doi.org/10.1016/s1006-706x(10)60099-4
3. Magudeeswaran G., Balasubramanian V., Madhusudhanreddy G. Hydrogen induced cold cracking studies on armour grade high strength, quenched and tempered steel weldments // International Journal of Hydrogen Energy. 2008. Vol. 33, Issue 7. P. 1897–1908. doi: https://doi.org/10.1016/j.ijhydene.2008.01.035
4. Demir T., Übeyli M., Yıldırım R. O. Effect of Hardness on the Ballistic Impact Behavior of High-Strength Steels Against 7.62-mm Armor Piercing Projectiles // Journal of Materials Engineering and Performance. 2009. Vol. 18, Issue 2. P. 145–153. doi: https://doi.org/10.1007/s11665-008-9288-3
5. Sampath K. How to Choose Electrodes for Joining High-Strength Steels // Welding Journal. 2007. P. 26–28. URL: https://app.aws.org/www/wj/2007/07/WJ_2007_07.pdf?_ga=2.143746806.298708127.1558695448-1529157542.1558695448
6. Messler R. W. Principles of Welding. John Wiley & Sons, 1999. doi: https://doi.org/10.1002/9783527617487
7. Krauss G. Martensite in steel: strength and structure // Materials Science and Engineering: A. 1999. Vol. 273-275. P. 40–57. doi: https://doi.org/10.1016/s0921-5093(99)00288-9
8. Effect of tempering conditions on wear resistance in various wear mechanisms of H13 steel / Wei M. X., Wang S. Q., Wang L., Cui X. H., Chen K. M. // Tribology International. 2011. Vol. 44, Issue 7-8. P. 898–905. doi: https://doi.org/10.1016/j.triboint.2011.03.005
9. Dziurka R., Pacyna J. The influence of carbon content on the kinetics of phase transformations of undercooled austenite of the Cr-Mn-Mo model alloys // Archives of Materials Science and Engineering. 2011. Vol. 47, Issue 2. P. 77–84.
10. Effect of Tempering Temperature on Microstructure and Properties of E690 Offshore Plate Steel / Zhang J., Cai Q., Wu H., Zhang K., Wu B. // Journal of Iron and Steel Research International. 2012. Vol. 19, Issue 3. P. 67–72. doi: https://doi.org/10.1016/s1006-706x(12)60076-4
11. Effect of tempering temperature, plate thickness and presence of holes on ballistic impact behavior and ASB formation of a high strength steel / Mishra B., Jena P. K., Ramakrishna B., Madhu V., Bhat T. B., Gupta N. K. // International Journal of Impact Engineering. 2012. Vol. 44. P. 17–28. doi: https://doi.org/10.1016/j.ijimpeng.2011.12.004
12. Effects of auto-tempering behaviour of martensite on mechanical properties of ultra high strength steel sheets / Matsuda H., Mizuno R., Funakawa Y., Seto K., Matsuoka S., Tanaka Y. // Journal of Alloys and Compounds. 2013. Vol. 577. P. S661–S667. doi: https://doi.org/10.1016/j.jallcom.2012.04.108
13. Persson E. Austenite grain growth in bearing steels. An investigation on steel grades 100Cr6 and 100CrMnMoSi8-4-6. Stockholm, 2014. 97 p.
14. Zdravecká E., Tkáčová J., Ondáč M. Effect of microstructure factors on abrasion resistance of high-strength steels // Research in Agricultural Engineering. 2014. Vol. 60, Issue 3. P. 115–120. doi: https://doi.org/10.17221/20/2013-rae
15. Variation of Creep Resistance in Ferritic Steels by a Heat Treatment / González G., Molina R., Delavalle M., Moro L. // Procedia Materials Science. 2015. Vol. 9. P. 412–418. doi: https://doi.org/10.1016/j.mspro.2015.05.011
16. Effects of tempering mode on the structural changes of martensite / Saha D. C., Biro E., Gerlich A. P., Zhou Y. // Materials Science and Engineering: A. 2016. Vol. 673. P. 467–475. doi: https://doi.org/10.1016/j.msea.2016.07.092
17. Ebrahimian A., Ghasemi Banadkouki S. S. Mutual mechanical effects of ferrite and martensite in a low alloy ferrite-martensite dual phase steel // Journal of Alloys and Compounds. 2017. Vol. 708. P. 43–54. doi: https://doi.org/10.1016/j.jallcom.2017.02.287
18. Hidalgo J., Findley K. O., Santofimia M. J. Thermal and mechanical stability of retained austenite surrounded by martensite with different degrees of tempering // Materials Science and Engineering: A. 2017. Vol. 690. P. 337–347. doi: https://doi.org/10.1016/j.msea.2017.03.017
19. Hosmani S. D., Kurhatti R. V., Kabadi V. K. Wear Behavior of Spherodized Cementite in Hyper Eutectoid Plain Carbon Steel // International Advanced Research Journal in Science, Engineering and Technology. 2017. Vol. 4, Issue 7. P. 257–262. URL: https://iarjset.com/upload/2017/july-17/IARJSET%2044.pdf
20. An atomic mechanism for the formation of nanotwins in high carbon martensite / Chen Y., Ping D., Wang Y., Zhao X. // Journal of Alloys and Compounds. 2018. Vol. 767. P. 68–72. doi: https://doi.org/10.1016/j.jallcom.2018.07.099
21. Wear investigation of selective α-Fe_2O_3 oxide layers generated on surfaces for dry sheet metal forming / Behrens B.-A., Yilkiran D., Schöler S., Özkaya F., Hübner S., Möhwald K. // Procedia Manufacturing. 2018. Vol. 15. P. 923–930. doi: https://doi.org/10.1016/j.promfg.2018.07.404
22. Laboratory team, 2019, Modul Praktikum Uji Aus (Indonesian). Mechanical Engineering Departement, Faculty of Engineering, Yogyakarta, Gadjah Mada University.
23. Soejanto, Irwan. Desain Eksperimen dengan Metode Taguchi. Yogyakarta, Graha Ilmu, 2009.
24. Krishnaiah K., Shahabudeen P. Applied Design of Experiments and Taguchi Methods. New Delhi, 2012. 371 p.